A preliminary measurement of the
fine structure constant based on atom interferometry

Andreas Wicht, Joel M. Hensley, Edina Sarajlic and Steven Chu

Physics Department, Stanford University, Stanford, CA 94305

Using an atom interferometer method, we measure the recoil velocity of cesium due to the coherent scattering of a photon. This measurement is used to obtain a value of $\hbar/M_{Cs}$ and the fine structure constant, α. The current fractional uncertainty is $\Delta\alpha/\alpha = 7.4 \times 10^{-9}$.

1. Introduction

The fine structure constant $\alpha = \mu_0 c e^2/2h$, where $\mu_0 = 4\pi \times 10^{-7}$ H/m is the permeability of the vacuum, c is the speed of light, e is the electron charge, and h is Planck s constant, sets the scale of electromagnetic interactions. Its importance is evidenced by the fact that it appears interwoven in many measurements of fundamental physical constants [1,2]. At present, the most accurate determinations of α span the domain of atomic physics, mesoscopic and macroscopic condensed matter physics, and elementary particle physics. Comparison of various accurate measurements of α constitute one of the most demanding tests of the consistency of physics. A summary of the most accurate determinations of α, along with our preliminary value from this work, is shown in Fig. 1. It is interesting to note that the 4 most accurate determinations of this constant follow directly from experimental work that have been awarded Nobel Prizes.

The fine structure constant can be written as

$$\alpha^2 = \left(\frac{2R_\infty}{c}\right)\left(\frac{m_p}{m_e}\right)\left(\frac{M_{Cs}}{m_p}\right)\left(\frac{h}{M_{Cs}}\right), \tag{1}$$

where the Rydberg constant R_∞ [1], and the mass ratios M_{Cs}/m_p [3], and m_p/m_e [1], have been determined with accuracies of 0.008, 0.20, and 2.1 ppb respectively. Thus, a measurement of h/M_{Cs} of comparable precision, in conjunction with the other measured quantities, yields an improved value of α.

2. Experimental method

We obtain a value of h/M_{Cs} by measuring the photon recoil velocity. Our method has been described in detail elsewhere [4,5,6]. The method we have developed is summarized as follows. Consider an atom moving with momentum **v** and in the ground state $|g\rangle$ that is excited by a π-pulse into excited state $|e\rangle$. The atom recoils with a velocity $v_{rec} = \hbar k/M$. Energy conservation determines the resonance condition

$$\omega - \omega_{eg} = \mathbf{k}\cdot\mathbf{v} + \hbar k^2/2M, \tag{2}$$

where ω_{eg} is the energy separating the states $|g\rangle$ and $|e\rangle$. If the recoiling atom is stimulated back down to the ground state by a counter-propagating photon of momentum $\hbar k'$, the resonance condition for this photon is

$$\omega' - \omega_{eg} = -\mathbf{k'}\cdot\mathbf{v} - \hbar\mathbf{k}\cdot\mathbf{k'}/M - \hbar k'^2/2M. \qquad (3)$$

The two frequencies ω and ω' are shifted by an amount

$$\omega - \omega' = (\mathbf{k} + \mathbf{k'})\cdot\mathbf{v} + (\hbar/2M)(\mathbf{k} + \mathbf{k'})^2. \qquad (4)$$

The term $\omega_{rec} = 2\pi f_{rec} \equiv \hbar k^2/M$ is defined as the recoil frequency and $v_{rec} \equiv \hbar k/M$ is the recoil velocity. Since the frequency of the light used to induce the transition has been accurately measured [7], ω_{rec} can be determined if the velocity of the atoms is known. The recoil shift appears as a spectral doublet in saturation absorption spectroscopy, which selects atoms with zero velocity with respect to counter-propagating laser beams [8].

The velocity dependent term in Eq. 4 can also be eliminated by replacing the 2 π-pulses with 2 pairs of $\pi/2$-pulses as shown in Fig. 2. This so-called Ramsey-Bordé interferometer was first used as an extension of the Ramsey method of separated oscillatory fields into the optical domain [9]. Since the sequence of 4 $\pi/2$-pulses creates two interferometers, the photon recoil measurement is transformed into a differential measurement of phase differences between two atom interferometers. This configuration has several advantages over a measurement based on two π-pulses. (*i*) The recoil shift is independent of the atom's initial velocity, the acceleration due to gravity, and *all* other shifts that are position independent (e.g. if the external reference oscillator is not set equal to ω_{eg}) because of the differential nature of the measurement. (*ii*) The frequency resolution is determined by the time between each pair of $\pi/2$-pulses while the duration of the $\pi/2$-pulses determines the spectral width of the pulses. Thus, by using fairly short $\pi/2$ pulses, a relatively large number of atoms in the atomic fountain can be addressed without sacrificing frequency resolution.

Using this interferometer configuration as a basic starting point, we improve the resolution of the measurement in several ways. (*i*) The precision of this interferometer is greatly increased by inserting N π-pulses between the two sets of $\pi/2$-pulses. These π-pulses increase the spatial separation of the end points of the two interferometers and have the effect of increasing the recoil frequency shift to $(N+1)\omega_{rec}$. (*ii*) The measurement time of the interferometer is extended by doing the experiment in an atomic fountain.[10] The atoms are launched with "moving molasses" where the polarization gradients in the optical molasses beams move with respect to the laboratory frame of reference.[11] The optimum time between $\pi/2$-pulses for our experiment is 0.12 seconds. (*iii*) In order to use the long measurement times made available with an atomic fountain, both atomic states should be stable against radiative decay. The ground and excited states are replaced by two ground states, and a two-photon Raman transition with counter-propagating beams is used to impart photon recoils with $\mathbf{k_L} \rightarrow \mathbf{k_{eff}} = \mathbf{k_1}$-$\mathbf{k_2}$, where $\mathbf{k_1}$, $\mathbf{k_2}$ are the wavevectors of the counter-propagating photons as defined in Fig. 3. The resulting Doppler-sensitive Raman resonance is determined by the microwave frequency difference between the two beams. Since this difference frequency can be phase locked to a stable microwave source, this method gives us twice the Doppler sensitivity of an optical transition with sub-milliHertz frequency resolution. (*iv*) Our current atom interferometer uses an adiabatic method of transferring momenta to the atoms first introduced by Gaubatz, *et al.* [12].

This form of adiabatic passage employs time-delayed and resonant light fields to efficiently transfer atoms between two states. By generating the time delayed pulses as shown in Fig. 3 with acousto-optic modulators, we were able to tailor the shape of the pulses to construct an atom interferometer [5]. The efficiency of the coherent transfer is ~94%, allowing us to measure the photon recoil with the two interferometers separated by 120 single photon momenta (N = 30 π-pulses).

A second benefit in switching from off-resonant Raman pulses [4] to adiabatic passage [5] is that the interferometer fringe contrast after many π-pulses is preserved. The adiabatic pulses use σ^+ polarized light tuned between the two 6 $S_{1/2}$, $|F=3, m_F = 0\rangle$ and $|F=4, m_F = 0\rangle$ ground states and the 6$P_{1/2}$, $|F'=3, m_{F'}= +1\rangle$ excited state. Atoms that are *not* coherently transferred fall into other Zeeman sublevels and most of them are optically pumped to the ground states $|4,+4\rangle$, $|4,+3\rangle$ and $|3,+3\rangle$ where they can no longer be excited by the σ^+ light tuned to the F'=3 level. The small fraction of atoms that fall incoherently back into the $|3,0\rangle$ or $|4,0\rangle$ states do not cause a net average phase shift.

We calculate the phase shift of each path of the atom interferometer using Feynman s path integral formulation of quantum mechanics [13]. In this formulation, the phase shift is divided into two contributions. The first contribution is due to the free evolution of the wavefunction $\Delta\Phi_{free} = S_{cl}/\hbar$, given by

$$S_{Cl}/\hbar = \frac{1}{\hbar}\int dt \left\{ \frac{1}{2}mv^2 - m[g + \delta g(z)]z(t) - \hbar\omega_i \right\}, \qquad (5)$$

where the integral is over the classical trajectory. The integrand (Lagrangian) includes terms due to the kinetic energy, the gravitational energy including a gravity gradient, and the internal energy state of the atom. In our measurement, the two interferometers are separated by ~5 cm and experience a ~8 ppb difference in the gravitational potential. This difference yields a ~10 ppb correction to the measured phase shift [14,15].

The second contribution to the phase shift is due to the interaction of the atoms with the optical field. In the short pulse limit, one can show [13] that for the transitions $|g\rangle \rightarrow |e\rangle$ and $|e\rangle \rightarrow |g\rangle$, there is an additional phase term exp[+i($k_{eff}z$ - $\omega_L t$ +ϕ_L)] and exp[- i($k_{eff}z$ - $\omega_L t$ +ϕ_L)], respectively, where k_{eff} is the effective k-vector of the Raman pulse, z is the position of the atomic wavefunction at time t, ω_L is the optical frequency, and ϕ_L any additional phase factor of the light. The terms k_{eff}, z, ω_L, and ϕ_L are all functions of time.
For the transitions $|g\rangle \rightarrow |g\rangle$ and $|e\rangle \rightarrow |e\rangle$, there is no added term.

The phase of each atom interferometer in Fig. 2 (with 30 added π-pulses) is measured in a manner analogous to the separated oscillatory field method due to Ramsey. In a Ramsey measurement, the phase difference between two states of the atom is compared to the phase of microwave oscillator. If the number of cycles of atomic phase that have accrued during the time between the π/2-pulses matches the number of cycles of phase of the microwave oscillator, an atom initially in state $|g\rangle$ is put in state $|e\rangle$. If the frequency of the microwave oscillator is scanned near the resonance condition, the atomic population oscillates between $|e\rangle$ and $|g\rangle$. The frequency difference between the two atomic states is determined by locating the center of this central Ramsey fringe.

In the case of our atom interferometer, the phase difference between the two arms is more complicated, as described above, but the principle is still the same. If the phase of the local oscillator tracks exactly the phase difference between the two arms of the interferometer, the atom originally in state $|g_1\rangle$ is returned back to its initial state. Any difference in phase accrued by the microwave oscillator and the two arms of the interferometer produces Ramsey oscillations between states $|g_1\rangle$ and $|g_2\rangle$. By determining the peak of the central fringe of the interferometer, we measure the ω_{rec} since this quantity limits the location of the central fringe relative to all other quantities such as the frequency of the light, the ground state hyperfine splitting, acceleration due to gravity, etc. This measurement requires a microwave oscillator whose frequency can be changed in a completely phase coherent manner.

The measurement is made less sensitive to experimental imperfections by measuring the phase difference between the two atom interferometers, $\Phi_1 - \Phi_2$. Systematic effects that are common to both interferometers are then subtracted out. A second pair of interferometers Φ_3, Φ_4 is created by reversing the directions of all the momentum impulses to create a pair of inverted interferometers. This inversion helps cancel spatially dependent systematic effects such as linear gradients in the bias magnetic field, non-linear frequency dependent electronic phase shifts, and laser frequency dependent phase shifts. The photon recoil frequency ω_{rec} is determined from the phase difference

$$\Delta\Phi = [(\Phi_1 - \Phi_2) + (\Phi_3 - \Phi_4)] = -8(N+1)(\omega_{rec} - \omega_{fixed})T - 4k_{eff}|\langle\delta g\rangle| (T+ T')T, \qquad (6)$$

where $|\langle\delta g\rangle|$ is the average difference in the gravitational potential for the two trajectories, and T' is time between the 2nd and 3rd $\pi/2$-pulses. The quantity, ω_{fixed} is the value assumed by the local oscillator. We set $\omega_{fixed} = 2\pi \times 15\,006.278\,875$ based on measurements before the 1998 adjustment of the fundamental constants [1]. The phase shift we measure then gives us the difference from the previously accepted value and the new value. In calculating the gravity gradient correction, we evaluate $|\langle\delta g\rangle|$ by using Eq. 5 to calculate the action S/.

2. Systematic effects

We have searched for a variety of systematic effects by varying many experimental parameters such as the time between the $\pi/2$-pulses, the number of π-pulses, the positions in the fountain trajectories where the light/atom interactions occur, the intensity and shape of the optical pulses. We have also changed the frequency offsets, polarization, alignment and wavefront curvature of the laser beams and varied environmental factors such as the magnetic bias field and density of hot cesium atoms. A preliminary discussion of potential systematic effects was given earlier [16]. We present here upper bounds on the systematic effects we have considered.

2.1 Beam alignment and wavefront curvature

We have developed an alignment procedure that can produce counter-propagating beams to within $\pm$ 15 µrad, corresponding to a 0.23 ppb error in $\omega_{rec} \sim (\mathbf{k} + \mathbf{k}')^2$. The optical alignment was observed to drift for about an hour after a re-alignment to roughly 1 ppb from the ideal alignment. For this reason we choose to correct all our data by 1 ppb with a $\pm$ 0.4 ppb estimated uncertainty in this correction.

Another systematic effect that has to be considered at this level of precision is the Gouy phase shift of a laser beam in the vicinity of the focal point, $\Phi_G = \arctan[\lambda z/\pi\omega_0^2]$, where ω_0

is the Gaussian beam radius [17]. For $\omega_0 = 1$ cm, this phase shift results in a 0.8 ppb correction in h/M for atoms centered at the waist of the 2 cm diameter beam. To ensure that the beams are correctly collimated, the positions of the 2m focal length lens was moved 2 to 4 centimeters away from the collimating position. The change in phase shift with the de-collimation was measured to be 1.4 ± 3.9 ppb per 1 cm of change in the position of the lens, whereas the lens can be set to ± 0.2 mm uncertainty with the use of a precision optical flat. Possible phase shifts due to the partial clipping of the Raman beams, optical defects of the mirrors, lenses and windows, and optical polarization imperfections were also found not be significant.

2.2. Frequency effects

A calculation of h/M from our measurement of the recoil shift requires that the momentum of the light used in the Raman pulses be accurately known. The optical pulses are tuned to the Cs D_1 transition, which has been measured with high accuracy [7]. The laser used in our experiment is locked to a cesium reference frequency cell, calibrated against the laser cooled atoms in the atomic fountain.

The center of the zero-order Ramsey fringe is found by scanning the frequencies of the final $\pi/2$-pulses. If there is a systematic offset in the tuning of the two-photon resonance, each of the interferometers will have displaced fringes. However, any detuning error will also produce the same phase error in the momentum reversed interferometer, and the final phase difference calculated using Eq. 6 is insensitive to this error. This cancellation was tested by varying the detuning of the final $\pi/2$-pulse by $\pm$ 20 kHz away from the known resonance. The measured dependence was -0.29 ± 0.71 ppb/kHz.

The two-photon frequency difference is determined to much higher accuracy. The microwave source used in the experiment is referenced to the atomic clock timing signals broadcast by the United States Naval Observatory and received using a frequency standard with a LORAN C input. The accuracy of this system is estimated to be better than 1 Hz out of 9.2 GHz.

The atoms accelerate due to gravity in the atomic fountain. This velocity change has to be properly accounted for in order to insure we are tuned correctly to the two-photon resonance. The value of g in an adjacent laboratory ~8 meters away, and at the same elevation, is known to an accuracy of 7 ppb [18]. Thus, we can safely assume that g is known in the h/M laboratory to better than 1 part in 10^5. By varying the value of g by $\pm 0.3\%$, we established an error less than ± 0.002 ppb. In our correction due to the gradient in g, we use the value $(2.93 \pm 10) \times 10^{-6}$ s^{-2}, also measured in the adjacent lab [18]. Because the gradient was not measured in the h/M lab, we have increased the assigned uncertainty to 10% of the gradient value. Errors due to Raman beam misalignment with respect to the vertical enter primarily as a Sagnac phase shift (See below).

2.3 Zeeman shifts

The atom interferometer uses the $m_F = 0$ magnetic sublevels of the cesium ground state. The bias field was set at 72 mG, but the field in the interferometer region had spatial variations of 1.5 mG, as measured using the atoms in the atomic fountain. To the extent that the normal and inverted interferometers trace out the same atomic trajectories, the interferometer phase shift $[(\Phi_1 - \Phi_2) + (\Phi_3 - \Phi_4)]$ will be insensitive to phase errors caused by the magnetic field. Data taken between 0 and 600 mG shows that there is no significant correction to non-compensated Zeeman shifts at the level of 2 ppb.

2.3 AC Stark shifts

Unequal AC Stark shifts in the two arms of the interferometer can shift the interference fringes. The AC Stark shifts of concern are of the form $\Omega^2/4\Delta$, where Ω is the Rabi frequency and Δ is the detuning of the light from resonance. No unaccounted change in the measured recoil velocity was observed as the laser frequencies were varied. The detuning studies establish an upper limit of 0.1 ppb uncertainty due to AC Stark shifts. As an independent, but weaker constraint, we note that a considerable amount of data was collected using adiabatic transfer pulses with intensities (and hence Ω^2) that differed by a factor of 4. No statistically significant difference in the recoil value was seen at the 11 ppb level.

The optical wave fronts used in the experiment are actively stabilized. A vibration-isolated platform is used to measure the beat note of the two Raman beams [19]. This beat note provides the feedback signal used to compensate for the vibrations of the optical mounts, air currents, etc. that introduce phase noise into the Raman beams. The frequency difference is kept phase-locked to a stable microwave reference.

The vibration isolation system used in this experiment requires a tracer beam that follows the same optical path as the Raman beams in order to detect any change of optical path length difference. The frequency of the tracer beam is chosen to be close enough to the frequency of the Raman beams to accurately monitor vibrational noise, but far enough detuned so that the AC Stark shifts are not a problem. The tracer beam was turned on 1.8 msec before each $\pi/2$ pulse so that the lock in the vibration isolation feedback system has enough time to settle. An AC Stark shift due to the tracer beam should subtract out of the final phase shift measurement since the shift would be common to the normal and inverted interferometers. To verify that there was no effect, we increased the intensity of tracer beam by a factor of 20 and left the tracer beam on all the time. With these changes, any AC Stark shift would be magnified by a factor of 6700. The photon recoil value remained the same to within 10 ± 25 ppb. Accounting for the enhancement factor, the tracer beam must contribute a shift of less than a 0.004 ppb.

2.4 Coriolis forces

Phase shifts may arise because the atom interferometer may have some spatial area due to misalignment of an atom trajectory with respect to the direction of the momentum impulses induced by the Raman pulses, as shown in Fig. 4. This area will cause a Sagnac phase shift $\Delta\phi = 2(M/\hbar)\mathbf{\Omega}\cdot\mathbf{A}$, where $\mathbf{\Omega}$ is the angular velocity of the earth and $\mathbf{A}$ is the enclosed area. If the transverse spread of velocities in the atomic fountain is symmetric with respect to the direction of the Raman pulses, this effect can be minimized. The effect is further decreased because the areas are equal so each pair of interferometers nearly cancels and the inverted pair further cancels the normal pair.

To verify the insensitivity to rotations, data were taken with intentionally misaligned launch and Raman beam directions. To further amplify any gyroscope effect, the entire experimental apparatus was rocked back and forth sinusoidially with maximum angular velocity ~19 times earth s rotation. With the systematic effect magnified in this way, we established an upper limit ± 1.0 ppb uncertainty due to Coriolis forces.

2.5 Missed photon kicks

A crucial ingredient in the precision of our measurement is the addition of N π-pulses in between the two sets of π/2-pulses. The experiment demands that all the atoms receive exactly N additional photon recoils, and a phase error will result if some of the atoms miss one or more momentum changing π-pulses.

If an atom were to miss a Doppler-sensitive π-pulse, it would be in the bright state at the beginning of the next pulse. The next π-pulse would then induce incoherent, single-photon transitions resulting in no net (averaged) phase shift in the interferometer. Also, since the frequency width of the π-pulses is on the order of the recoil shift, an atom missing two or more π-pulses would be far enough off-resonance that it would not be affected by succeeding π-pulses.

The most serious concern is that some of the atoms may experience a Doppler-free transition induced by two *co*-propagating beams, where one of the beams is due to a reflection from an optical surface. To minimize the number of missed recoils from back reflections, we tilt all the optics in the near vicinity of the vacuum can. We also avoid illuminating the atoms with π-pulses close to the apogee of their trajectory where they would be most sensitive to Doppler free transitions.

An atom that misses one momentum impulse will be drastically shifted in phase by $\Delta\phi = (\hbar k^2_{eff}/M_{Cs})T$. If the fraction of atoms that miss a pulse is small, we can choose the time T so that $\Delta\phi$ is modulo 2π. With this choice of T, the fringe pattern with a small number of missed recoils will be the same as the fringe pattern with no missed recoils.

As a check on our ability to eliminate the chance of missed photon kicks, 30 π-pulses were added near the apogee of the atomic trajectory so that the laser would have a 100× higher probability of exciting a Doppler-free transition as compared to normal operating conditions. We then scanned the time interval T over a range where $\Delta\phi$ changed by 2π. The phase shift observed had an amplitude of 17 ± 16 ppb, which is consistent with no phase shift. Because of the enhancement factor of 100, we place a 0.16 ppb uncertainty on this error.

2.6 Phase shifts due to digitization errors

Every time an atom makes a transition between internal states, the position of the atoms with respect to the wavefront of the light is recorded onto the atomic wavefunction with an additional phase factor $\exp[\pm i(k_L z - \omega_L t + \phi_L)]$. The laser frequency must be shifted to keep the transition in resonance to compensate for the Doppler-shift because of the acceleration due to gravity and the photon recoil impulses. In the experiment, the laser difference frequency is shifted while the sum frequency is kept constant. In the process of shifting the laser frequency, however, the phase shifts in the electronics can be frequency-dependent, leading to errors in the measurement. In the thesis work of B. Young [6], this systematic effect was on the order of 100 ppb. Since this effect was discovered, we switched to a higher bandwidth frequency synthesizer with no rf filters on the output. The electronic frequency dependent phase shift was greatly decreased and the residual shift is 0.0 ± 0.2 ppb.

2.7 Phase errors due to π/2 pulses

If there is a phase error introduced by the π/2-pulses that is independent of the time T between π/2-pulses, then the phase difference between a pair of atom interferometers (neglecting the gravity gradient term) will vary as

$$\Delta\Phi = \Phi_1 - \Phi_2 = -4\pi (N+1)(\omega_{rec} - \omega_{fixed})T - \phi_{err} . \tag{8}$$

Thus, if the phase shift $\Delta\Phi$ is measured as a function T, a linear dependence in phase shift is expected. The slope of the line, $-4\pi(N+1)(\omega_{rec} - \omega_{fixed})$, yields the recoil velocity and the intercept at T=0 measures the phase shift error.

Fig. 5 shows the phase difference $\Phi_1 - \Phi_2$ plotted for data taken under two conditions. Curve (a) represents data taken while two independent acousto-optic modulators (AOMs) were used to shape the Raman pulses. The AOMs and the rf attenuators have been shown to add phase shifts to the laser light [16]. If the two Raman beams were turned off with separate AOMs and driving electronics, independent drifts in the phase shifts would appear in the phase of the atomic superposition state. The offset, ϕ_{err}, was reduced by adding an additional AOM that turned both laser beams off simultaneously. With this change, the value of ϕ_{err} became consistent with zero, as shown in curve (b).

The determination ω_{rec} from the slope of Eq. 8 is one of our most powerful controls over potential systematic effects. The analysis eliminates a large number of systematic shifts introduced by (*i*) non-ideal RF electronics used to generate the Raman pulses, (*ii*) the AOMs used to tailor the pulses, (*iii*) various phase locked loops affected by the switching of frequencies, and other electronic interference from rapid changes in the RF or optical intensities, (*iv*) pulsing MOT coils that might affect the vibration isolation platform. Our value of the photon recoil frequency is based on this data analysis method.

2.8 Index of refraction effects

Cs atoms in the vacuum chamber will produce a non-unity index of refraction for the light. This will change $k_{eff} = k + k'$, which will affect the recoil measurement by (*i*) changing the momentum imparted to the atoms by the light and (*ii*) by changing the phase difference $k_{eff}\Delta z$, where Δz is the separation between the two interferometers. Any shift in the recoil measurement due to room temperature Cs atoms has been shown to be less than 0.06 ppb by varying the pressure of Cs in the vacuum chamber.

The contribution from the cloud of cold atoms is more complicated. In addition to the usual dispersive features defined by the 5 MHz wide absorption of the other D_1-lines, there are much sharper dispersive features due to electromagnetically induced transparency effects. [20] The width of the induced transparency dip is defined by the linewidth of the adiabatic π-pulses and is ~ 200 kHz. Transitions between the $|F=4, m_F=0\rangle$ and the $|F=3, m_F=0\rangle$ states are made with light tuned exactly to the $|F'=4, m_F=+1\rangle$ excited state, so that the index of refraction for this transition remains 1 despite the sharp dispersive feature. However, the adiabatic pulses are only ~94% efficient, and therefore, other Zeeman ground states become populated. The population of these other states, specifically the $|F=4, m_F=+1, +2\rangle$ and $|F=3, m_F=+1, +2\rangle$ ground states will contribute to a non-zero effect since transitions to the excited states are tuned 50 and 100 kHz from resonance in a bias field of 72 mG.

After we became aware of this potential systematic effect, we determined an experimental upper limit to the dispersive effect by taking recoil data, switching between high and low atom densities with each succeeding launch. The number of atoms was reduced by a factor of 4 from normal operating conditions by collecting atoms in the MOT before launching for less time. The recoil value taken with the reduced density shifted by +7.3 ± 10.5 ppb,

consistent with no effect. The dispersive effect is linear with atomic density, so this measurement places an upper limit to the density dependent effects of $(7.3 \pm 10.5)(4/3)$ ppb.

3. Summary of systematic effects

A summary of the systematic effects that were considered is given in Table 1. Most upper limits to the uncertainties are experimentally determined. Some systematic effects that were considered, but not discussed here are also entered in Table 1. In the cases where the experimental test is consistent with zero and there are good reasons why there should not be a systematic effect when the parameter is varied, the uncertainty is kept, but no correction is applied to the value of ω_{rec}. The significant uncertainties (greater than 0.4 ppb) listed in Table 1 are added in quadrature.

The largest uncertainty in Table 1 is the experimentally determined uncertainty on possible density dependent effects. We have also analyzed this effect numerically using the optical Bloch equations that describe the time evolution of all the Zeeman sub-levels of the $S_{1/2}$ F=3 and F=4 ground states and the $P_{1/2}$ F′=3 excited states of cesium. The calculation shows that the effect due to index of refraction changes is less than 1ppb. In this paper, we include the experimentally determined uncertainty in our preliminary value of α, pending further verification of our calculations. However, because we expect that there will be no correction larger than 1 ppb to our final result, so we have not included a 9.7 ppb correction to our value of f_{rec}.

4. The value of h/M$_{Cs}$ and α

The preliminary value of α is determined from photon recoil measurement derived from data that measures the slope of the recoil shift versus T. The weighted average of 31 data sets of the type shown in Fig. 5 is $f_{rec} = f_{fix} [1 - (124.98 \pm 4.88) \times 10^{-9}]$. The chi-square is $\chi^2/(N-2) = 1.5$. This value of f_{rec} is adjusted by the values listed in right hand column of Table 1. In frequency units,

$$f_{rec} = 15\ 006.276\ 88\ (23)\ (7)\ (22), \tag{9}$$

where the quantities in parentheses are the total (15 ppb), the statistical (4.9 ppb), and systematic (14 ppb) uncertainties. Without the density dependent uncertainty, the systematic error in h/M reduces to 3.2 ppb. The other measurements needed to determine α based on Eq. 1 are given in Table. 2. Note that all the uncertainties are reduced by a factor of two when used to calculate α.

With these values, we arrive at a preliminary value for α^{-1} is

$$\alpha^{-1} = 137.036\ 000\ 3\ (10). \tag{10}$$

We are currently undergoing another review of our data analysis and numerical simulations of the atom interferometer using the optical Bloch equations. If the initial results are verified, we should be able to reduce uncertainty to α to 3.1 ppb. The h/M$_{Cs}$ contribution to this uncertainty is α to 2.9 ppb.

Table 1. Systematic error budget

Systematic effect	Experimental limit (ppb)	Theoretical limit (ppb)	Correction to h/M (ppb)
Optical beams			
Gouy phase shift		- 0.89 ± 0.04	+ 0.89 ± 0.4
Wavefront curvature	+ 0.035 ± 0.039	< 0.04	
Speckle			
Relative angle	- 1.0 ± 0.4		+1.0 ± 0.4
Beam clipping	+ 0.04 ± 0.04		
Polarization	± (1.5 ± 2.0)		±2.0
Magnetic fields			
Linear term	-1.0 ± 2.0		0 ± 2.0
Quadratic term	+0.15 ± 0.1		- 0.15 ± 0.1
Electric fields			
dc Stark effect		$< 2 \times 10^{-4}$	
ac Stark effect from tracer laser beam	< 0.004	< 0.008	
ac Stark effect from Raman lasers	0.016 ± 0.10		
Frequencies			
Lock to cesium		< 0.6	
Difference frequency	< 0.002		
Frequency switching	< 0.4		0 ± 0.4
Gravity chirp		< 0.002	
Gravity gradient			- 9.7 ± 1.0
Bad frequencies		0	
Computer arithmetic		0	
Dispersion			
cold atoms	-9.7 ± 14	In progress	0 ± 14
Hot background atoms		< 0.06	
Timing			
Line noise		0	
Synchronized fluctuations		<0.2	
Time resolution		0	
Other			
Missed recoils	< 0.16		
Sagnac effect from launch misalignment	< 0.3		
Sagnac effect from beam misalignment	< 1.0		0 ± 1.0
Collisional shifts		< 0.3	
π/2 pulses	See Fig. 8		

Table 2. Quantities use to determine α

Quantity	Value	Precision	Source
R_∞	10 973 731.568 549 (83) m^{-1}	0.0076	ref. 1
Cesium transitions			ref. 2
$F = 3 \rightarrow 3'$	335 120 562 838 (43) kHz	0.13 ppb	
$F = 4 \rightarrow 3'$	335 111 370 206 (43) kHz		
M_{Cs}	132.905 451 931 (27) amu	0.20 ppb	ref. 3
m_p	1.007 276 466 88 (13) amu	0.13 ppb	ref. 1
m_e	5.485 799 110 (12) $\times 10^{-4}$ amu	2.1 ppb	ref. 1
CODATA α^{-1}	137.035 999 76 (50)	3.7 ppb	ref. 1
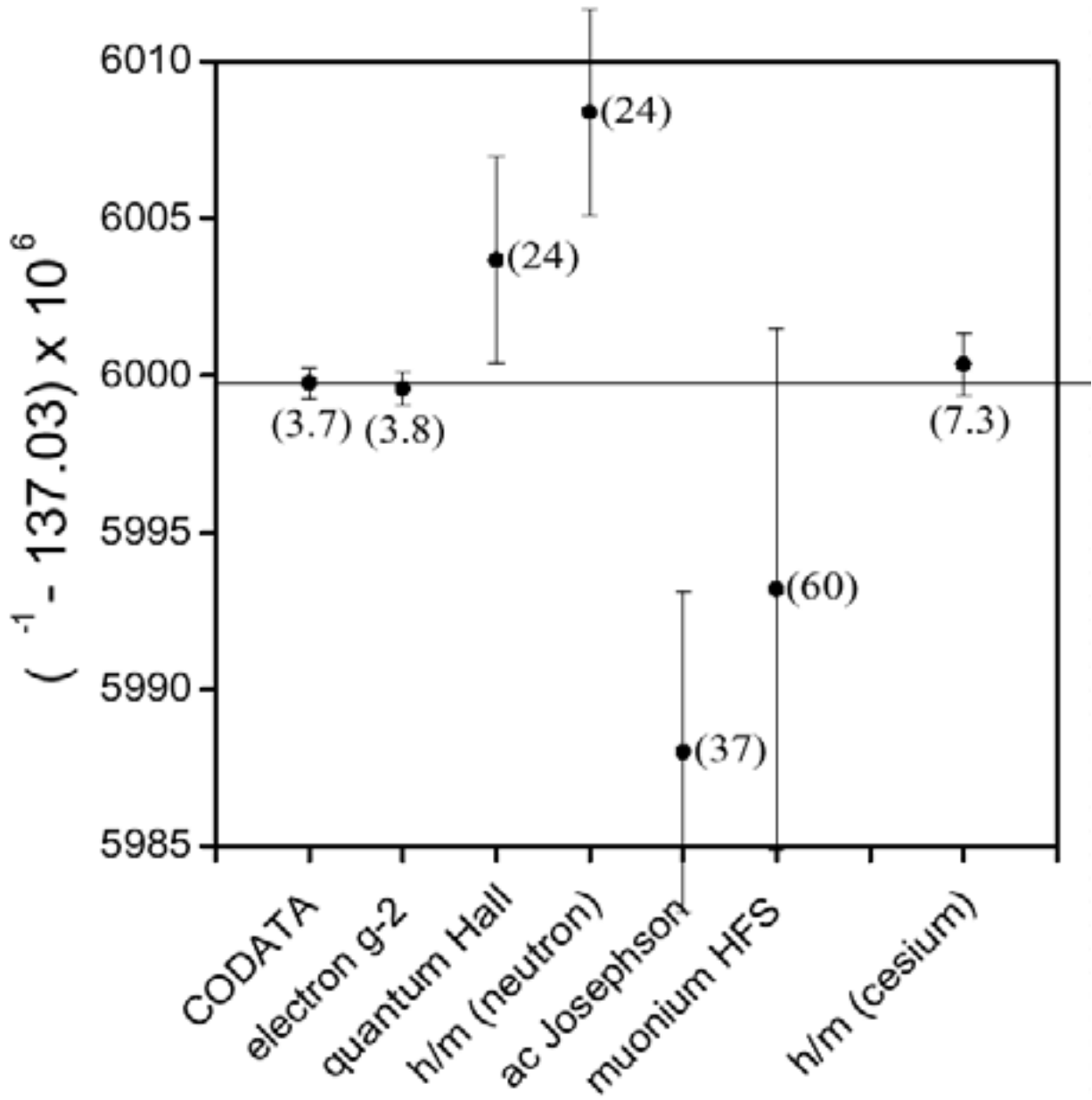
Fig. 1. Determinations of the fine structure constant α taken from Table XV of ref. 1 is shown with the CODATA value and our preliminary value. The neutron and muonium values are an average of several independent measurements.
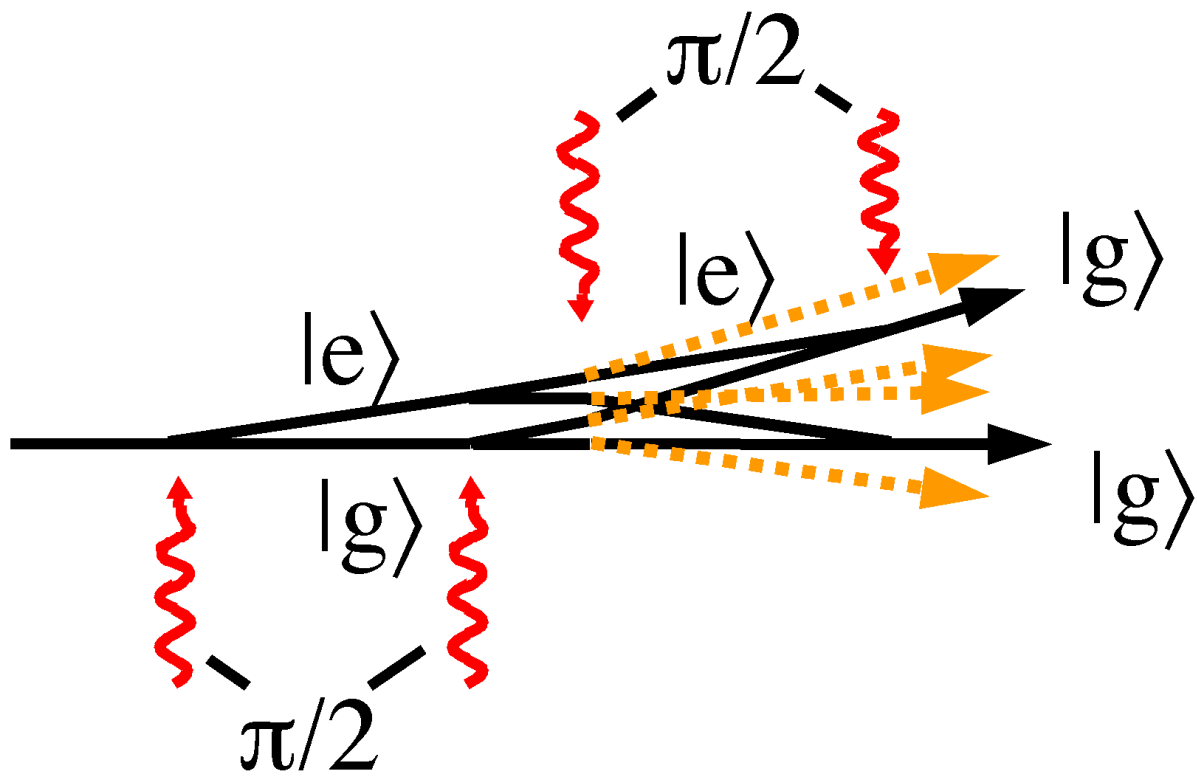
Fig 2. A space-time trajectory of a Ramsey-Bordé interferometer beginning with an atom initially at rest. Each arrow indicates the direction of the k-vector of the π/2-pulses. The dotted lines show atomic paths that do not contribute to the interference signal.
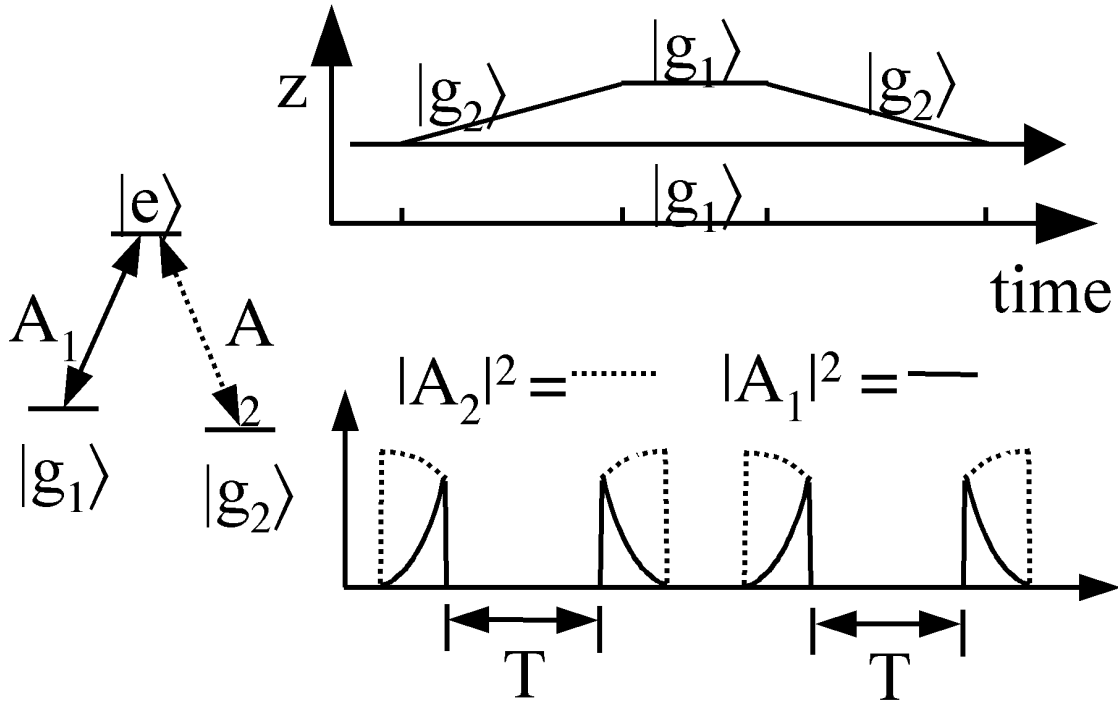
Fig 3. An atom interferometer based on adiabatic transfer between ground states $|g_1\rangle$ and $|g_2\rangle$. The upper diagram is a space-time diagram of the lower interferometer of Fig. 2. The intensity profiles of the pulses used to produce $\pi/2$ transitions for this interferometer are shown. In order to create the upper interferometer, the shapes of A_1 and A_2 are changed as indicated. In this figure, k_1 (k_2) is directed upward (downward.)
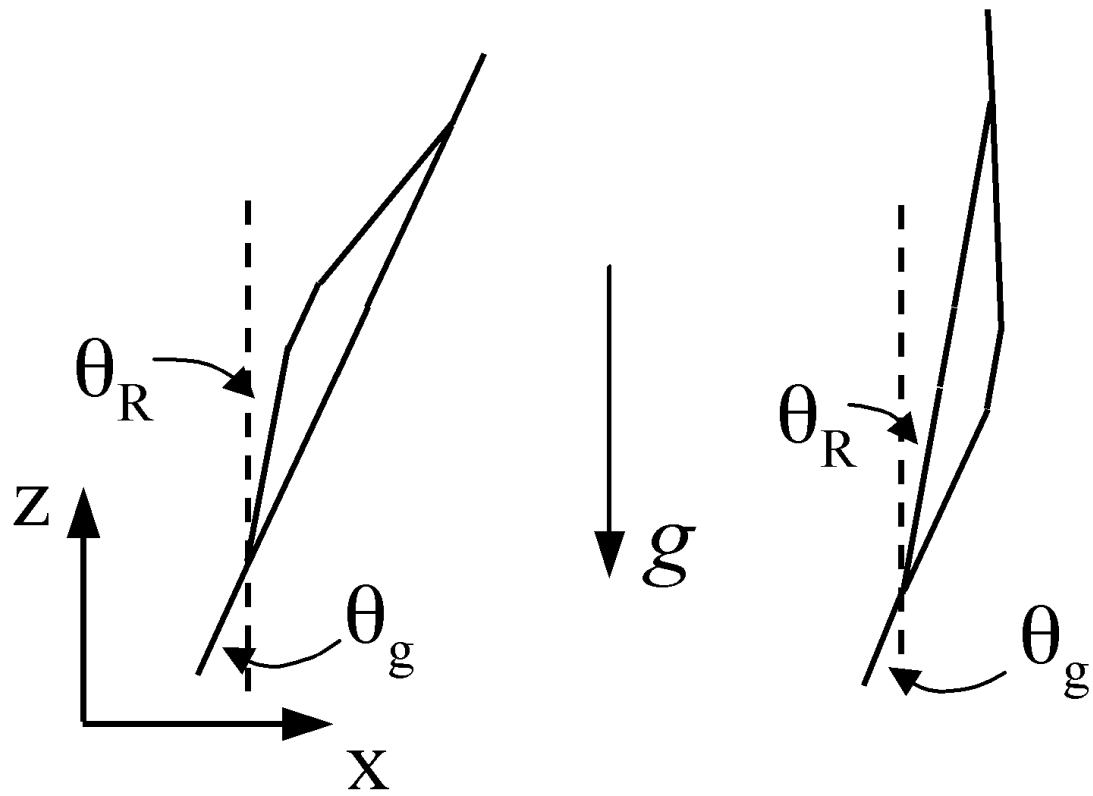
Fig. 4. The spatial areas enclosed by the two Ramsey-Bord interferometers due to a misalignment of the Raman beams θ_R or the launch θ_L with respect to gravity, g. The areas of the two interferometers are equal so that $\Phi_1 - \Phi_1 \sim 0$.
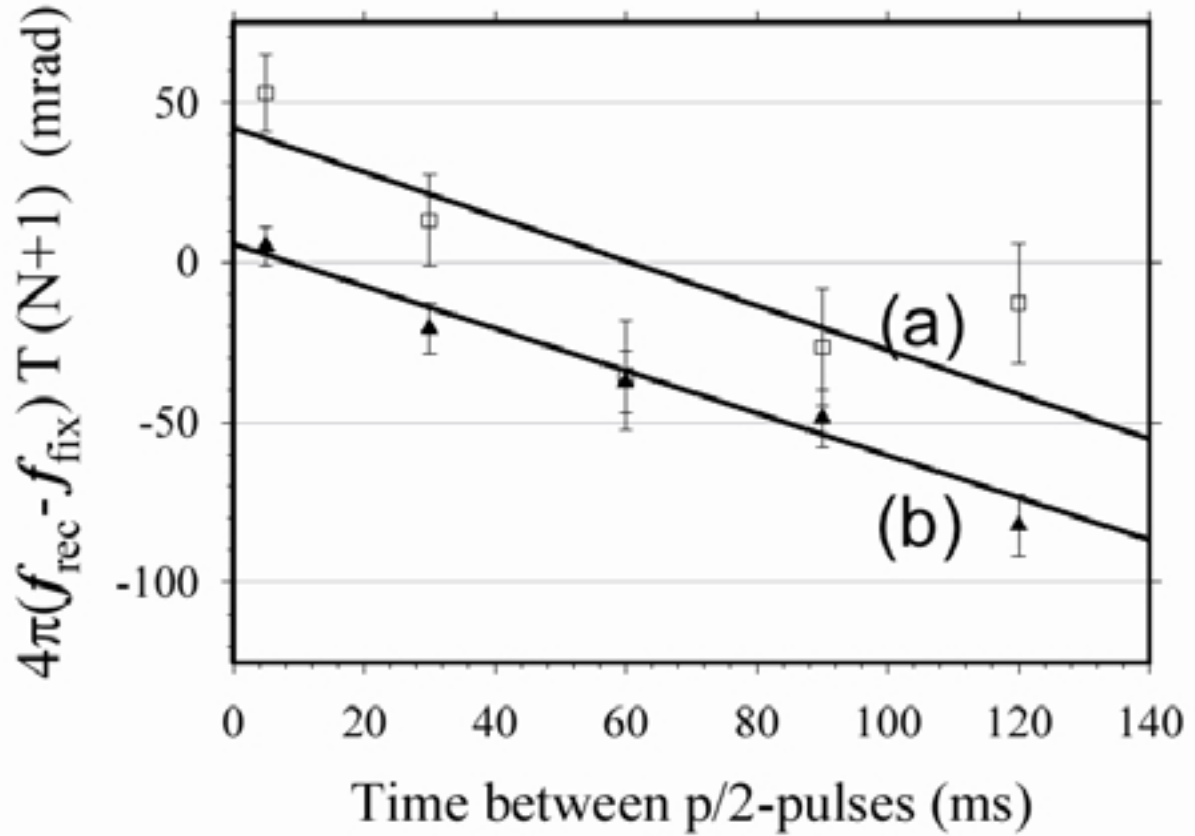
Fig. 5. The interferometer phase difference $\Delta\Phi = \Phi_1 - \Phi_1$ versus the time T between the $\pi/2$ pulses. This data was taken with 30 π pulses sandwiched in between the two sets of $\pi/2$ pulses. Pulse shaping AOMs are controlled by microwave attenuators that introduce attenuation dependent phase shifts. There are additional phase shifts which are due to thermal effects in the AOM. Unfortunately, even with the common acousto-optic modulator (AOM) installed, long term drifts in ϕ_{err} were still observed.

References

[1] P. J. Mohr and B. N. Taylor, CODATA recommended values of the fundamental constants: 1998, *Rev. Mod. Phys.* **72**, 351-495 (2000).

[2] T. Kinoshita, The fine structure constant, *Rep. Prog. Phys.* **59** 1459-1492 (1996).

[3] M. P. Bradley, *et al.*, Penning trap measurements of the masses Cs-133, Rb-87, Rb-85, and Na-23 with uncertainties ≤ 0.2 ppb, *Phys. Rev. Lett.* **83** (1999) 4510-4513.

[4] D.S. Weiss, B.C. Young, and S. Chu, *Phys. Rev. Lett.* **70**, 2706-2709 (1992); A*ppl. Phys. B* **59,** 217-256 (1994); M. Weitz, B.C. Young, and S. Chu, *Phys. Rev. A* **50**, 2438-2566 (1994); *Phys. Rev. Lett.* **73,** 2563-2566 (1994).

[5] M. Weitz, B.C. Young, and S. Chu, *Phys. Rev. A* **50**, 2438-2566 (1994); *Phys. Rev. Lett.* **73,** 2563-2566 (1994).

[6] B.C. Young, unpublished Ph.D. thesis, (1997); S. Chu, Les Houches Lectures in Physics, Session LXII, eds. R. Kaiser, C. Westbrook, and F. David, (Springer, Berlin, 2001) pp 317-370.

[7] T. Udem, J. Reichert, R. Holzwarth, T. W. H nsch, Absolute optical frequency measurement of the cesium D-1 line with a mode-locked laser, *Phys. Rev. Lett.* **82,** 3568-3571 (1999).

[8] J.L. Hall, Ch. J. Bord , and K. Uehara, Direct optical resolution of the recoil effect using saturated absorption spectroscopy. *Phys. Rev. Lett.* **37**, 1339-1342 (1976).

[9] Ch. J. Bordé Atomic interferometry with internal state labeling, *Phys. Lett. A* **140**, 10-12 (1989).

[10] M.A. Kasevich, E. Riis, S. Chu, and R.G. DeVoe, Rf Spectroscopy in an Atomic Fountain, *Phys. Rev. Lett.* **63**, 612 (1989).

[11] D.S. Weiss, E. Riis, M. Kasevich, K.A. Moler, and S. Chu, The Production and Uses of Slow Atomic Beams, in *Light Induced Kinetic Effects on Atoms, Molecules, and Molecules*, eds. L. Moi, S. Gozzini, C. Gabbanini, E. Arimondo, F. Strumia, (ETS Editrice, 1991) pp. 35-44.

[12] U. Gaubatz, *et al.*, *Chem. Phys. Lett.* **149**, 463 (1988).

[13] We first used this formalism in M. Kasevich and S. Chu, Atomic interferometry using stimulated Raman transitions, *Phys. Rev. Lett.* **67**, 181-183 (1991). Also see P. Storey and C. Cohen-Tannoudji, *J. Phys. II France* **4**, 1999-2027 (1994) for a good tutorial of this calculation.

[14] We are indebted to M. Kasevich for pointing out that this systematic effect does not subtract away in our experiment.

[15] A. Peters, K.Y. Chung and S. Chu, High precision gravity measurements using atom interferometry, *Metrol.* **38**, 25-61(2001).

[16] Joel Hensley, Andreas Wicht, Brent Young, and Steven Chu, Progress towards a Measurement of h/M, *Atomic Physics 17, Proceedings of the 17th Int. Conf. on Atomic Physics*, eds. E. Arimondo, P. De Natale, and M. Inguscio (AIP, Melville, New York, 2000) pp 43-57.

[17] H. Kogelnik and T. Li, *Appl. Opt.* **5**, 1550 (1966); A.I. Siegman, *Lasers*, University Science Books, Mill Valley, CA, 1986.

[18] A. Peters, K.-Y. Chung and S. Chu, An Measurement of Gravitational Acceleration by Dropping Atoms, *Nature* **400**, 849-852 (1999).

[19] J.M. Hensley, A. Peters and S. Chu, Active low frequency vertical vibration isolation. *Revs. of Sci. Inst.* **70**, 2735-2741 (1999).

[20] K. J. Boler, A. Imamogulu, and S. E. Harris, Observation of electro-magnetically induced transparency. *Phys. Rev. Lett.* **66**, 2593-2596 (1991).